Pattern-forming instabilities in nematic liquid crystals under oscillatory Couette flow

O. S. Tarasov,[1] A. P. Krekhov,[1,2] and L. Kramer[2,*]
[1]*Institute of Molecule and Crystal Physics, Russian Academy of Sciences, 450075 Ufa, Russia*
[2]*Physikalisches Institut, Universität Bayreuth, D-95440 Bayreuth, Germany*
(Received 30 May 2005; published 22 September 2005)

We consider instabilities, either homogeneous or periodic in space, which develop in a nematic liquid crystal layer under rectilinear oscillatory Couette flow for planar surface alignment of the director perpendicular to the flow plane. On the basis of a numerical and analytical linear stability analysis we determine the critical amplitude of the oscillatory flow, the wave number, and the symmetry of the destabilizing mode and present a comprehensive phase diagram of the flow instabilities. In particular it is found that by varying the frequency of the Couette flow the instability changes its temporal symmetry. This transition is shown to be related to the inertia effects of the nematic fluid, which become more important with increasing flow frequency. We also show that an electric field applied perpendicularly to the nematic layer can induce an exchange of instabilities with different spatial and temporal symmetries. The theoretical results are compared with experiments, when available.

DOI: 10.1103/PhysRevE.72.031709 PACS number(s): 61.30.Gd, 64.70.Md, 47.20.−k

I. INTRODUCTION

Nematic liquid crystals (nematics) represent one of the simplest anisotropic fluids [1]. In order to describe the macroscopic dynamics of these materials made up from elongated molecules one needs, in addition to the velocity and pressure field, an additional hydrodynamic variable, the *director* field $\boldsymbol{n}$, which is parallel to the direction of the preferred local molecular orientation. The strong coupling between the director and the velocity fields provides a number of interesting pattern forming instabilities in nematics under flow [2–5]. The flow behavior of a nematic strongly depends on the geometry and material parameters, in particular on the sign of the ratio of the Leslie viscosity coefficients α_3 and α_2. For materials with rodlike molecules α_2 is negative, whereas the sign of α_3 is not restricted *a priori*. If the nematic is initially oriented within the flow plane, i.e., within the plane spanned by the velocity of the primary flow and its gradient, then under rectilinear *steady* flow (of Couette or Poiseuille type) in materials with $\alpha_3<0$ the director remains within the flow plane. It includes an angle $\theta_{\mathrm{fl}}=\arctan\sqrt{\alpha_3/\alpha_2}$ with the flow direction according to a well known stationary homogeneous solution of the nematodynamic equations [1,6]. This solution θ_{fl} (with appropriate sign of the square root) is linearly stable in the case of steady flows [6–8]. These nematics are called "flow aligning." In oscillatory flows the director tends to oscillate between the angles $\pm\theta_{\mathrm{fl}}$. With a nonlinear velocity profile, like in Poiseuille flow, this oscillatory solution can lose stability [9,10].

In contrast, for $\alpha_3>0$ under steady flow the stationary solution θ_{fl} does not exist and one has tumbled regime with a director profile depending strongly on the shear rate [4]. Nematics with $\alpha_3>0$ are called "non-flow-aligning."

The phenomena of orientational transitions becomes even richer if the director is initially oriented perpendicular to the flow plane. This situation corresponds, for symmetry reasons, to a stationary homogeneous solution of the nematodynamic equations. In the classical work by Pieranski and Guyon (PG), however, it was shown that in the absence of additional torques from bounding surfaces or external fields this solution is unstable for $\alpha_3<0$ [11]. In confined geometry, which sets a certain length scale in the system, the solution loses stability only above some critical value of the shear rate via a stationary bifurcation [11,12]. Henceforth, we concentrate on the case with negative α_3. In steady Couette as well as Poiseuille flows the unstable mode is homogeneous in space, i.e., the critical wave number is $q_c=0$.

The situation changes in the presence of external fields. In steady Couette flow stabilizing magnetic field (for usual nematics the anisotropy of the magnetic susceptibility is positive) above critical strength applied along the initial director orientation changes the type of instability from homogeneous to spatially periodic ($q_c\neq 0$) leading to a roll pattern [11]. In steady Poiseuille flow stabilizing magnetic field does not affect the type of instability [12], but rolls can be observed above a secondary instability [12].

In oscillatory Couette flow experiments of PG [11] in the frequency range 0.5–2.5 Hz and recent experiments [13,14] for frequencies $f\leqslant 150$ Hz show the appearance of a roll instability with the critical shear rate depending on the flow frequency. The temporal symmetry of the instability is influenced by an applied electric field stabilizing the orientation in the plane of nematic layer (negative anisotropy of the dielectric permittivity) [11]. A theoretical treatment of the problem [2,11,15,16] gives the mechanisms of the instability and is in a good agreement with experimental results, including the change in symmetry. For oscillatory Poiseuille flow the situation is similar [17–19]. In all the theoretical treatments [2,15,16] the inertia of the fluid is neglected, which is reasonable for low frequencies of the applied shear flow, i.e., when the (circular) flow frequency ω is much less than the inverse of the viscous relaxation time $\tau_v\sim\rho d^2/\eta$ (ρ is the nematic liquid crystal density, d is a thickness of nematic

*Deceased.

layer and η an effective viscosity of the nematic). In the absence of an electric field one then has no changes in the instability scenario with the flow frequency.

In the present work we investigate numerically as well as analytically homogeneous and spatially periodic instabilities induced by plane, oscillatory Couette flow with the director prealigned perpendicular to the flow plane in a wide range of the flow frequencies (up to $\omega \sim \tau_v^{-1}$, which is about 10^4 s^{-1} for typical thickness of the nematic layer $d \sim 100$ μm). Furthermore, we study the influence of an electric field on the flow instabilities for negative and positive anisotropy of the dielectric permittivity of the nematic. Special attention is given to the regimes with high flow frequencies ($\omega\tau_v \sim 1$), where the present experimental data lack precision. It is worth noting that recent experiments [13,14] demonstrate techniques to study the high-frequency range in detail and to improve the experiments.

In Sec. II we present the formulation of the problem based on the standard set of Leslie-Ericksen nematodynamic equations [1,6] and explain the numerical procedure used for linear stability analysis. In Sec. III the results of the stability analysis are given and compared with available experimental data. Finally, in Sec. IV we draw our conclusions and put the results into perspective.

II. GOVERNING EQUATIONS AND STABILITY ANALYSIS

We consider a nematic layer bounded by two infinite parallel plates at $z=\pm d/2$ with the z axis perpendicular to the plates. The upper plate (at $z=d/2$) is oscillated harmonically along x with an amplitude A and a (circular) frequency $\omega = 2\pi f$. The director is oriented (rigidly anchored) at the boundaries along y axis. An additional electric field of strength E can be applied along z axis. It is convenient to introduce the dimensionless variables

$$\tilde{\boldsymbol{r}} = \boldsymbol{r}/d, \quad \tilde{t} = t\omega, \quad a = A/d. \tag{1}$$

Henceforward we omit the tildes.

For small amplitude A/d the system remains in the basic state, i.e., the director is undistorted and the nematic behaves like an isotropic fluid with the viscosity $\eta_3 = \alpha_4/2$, where α_i are the Leslie viscosity coefficients [1,6]. The basic state is calculated as homogeneous solution of the standard set of nematodynamic equations (Leslie-Ericksen equations [1,6])

$$\boldsymbol{n}^0 = (0,1,0), \quad \boldsymbol{v}^0 = (v_x^0(z,t),0,0). \tag{2}$$

The velocity profile can be found from Navier-Stokes equation

$$\epsilon_v \partial_t v_x^0 = \partial_z^2 v_x^0, \quad v_x^0|_{z=1/2} = a\cos t, \quad v_x^0|_{z=-1/2} = 0. \tag{3}$$

Here the notations $\partial_t = \partial/\partial t$, $\partial_z = \partial/\partial z$, $\partial_z^2 = \partial^2/\partial z^2$ and so on are used and

$$\epsilon_v = \omega\tau_v, \quad \tau_v = \rho d^2/\eta_3, \tag{4}$$

with τ_v the viscous relaxation time which is typically of order 10^{-4} s (for $\rho \sim 10^3$ kg/m^3, $d \sim 100$ μm and $\eta_3 \sim 10^{-1}$ N s/m^2).

In order to investigate the stability of Eq. (2) we linearize the nematodynamic equations [1,6] around the basic state as follows:

$$\boldsymbol{n} = (0,1,0) + (n_x,n_y,n_z),$$

$$\boldsymbol{v} = (v_x^0,0,0) + (v_x,v_y,v_z), \tag{5}$$

where the perturbations $n_i = n_i(y,z,t)$, $v_i = v_i(y,z,t)$, $\{i = x,y,z\}$ are small. Guided by the experimental observations we assume that the wave vector of the destabilizing modes, if not zero, is perpendicular to the flow plane.

It follows from the director normalization equation $\boldsymbol{n}^2 = 1$ that $n_y \equiv 0$ in linear approximation. Eliminating v_y by use of the incompressibility condition $\partial_y v_y = -\partial_z v_z$ and the pressure by taking the *curl* of the Navier-Stokes equation one obtains for (v_x, v_z, n_x, n_z)

$$(\epsilon_v \hat{L}_1 - \hat{L}_2) v_x = -\epsilon_v v_{x,z}^0 \partial_y v_z + \alpha_2' \partial_t \partial_y^2 n_x + \frac{1}{2}(-\alpha_2' + \alpha_5') v_{x,z}^0 \partial_y^2 n_z, \tag{6}$$

$$(\epsilon_v \hat{L}_3 - \hat{L}_4) v_z = \frac{1}{2}(\alpha_2' + \alpha_5') v_{x,z}^0 \partial_y^3 n_x - \frac{1}{2}(\alpha_3' + \alpha_6') \partial_z^2 (v_{x,z}^0 \partial_y n_x) + \alpha_2' (\partial_y^2 - \lambda \partial_z^2) \partial_t \partial_y n_z, \tag{7}$$

$$(1-\lambda)(\partial_t - \epsilon_d \hat{G}_1) n_x = v_{x,z}^0 n_z + \partial_y v_x, \tag{8}$$

$$(1-\lambda)(\hat{L}_1 - \epsilon_d \hat{G}_2) n_z = \lambda v_{x,z}^0 \partial_y n_x + (\partial_y^2 - \lambda \partial_z^2) v_z, \tag{9}$$

with $v_{x,z}^0 = \partial_z v_x^0$. The $\hat{L}_i$ and $\hat{G}_i$ are linear differential operators

$$\hat{L}_1 = \partial_t \partial_y, \quad \hat{L}_2 = \partial_y(\eta_2' \partial_y^2 + \partial_z^2), \quad \hat{L}_3 = \partial_t(\partial_y^2 + \partial_z^2),$$

$$\hat{L}_4 = \eta_2' \partial_y^4 + (\alpha_1' + \eta_1' + \eta_2') \partial_y^2 \partial_z^2 + \eta_1' \partial_z^4,$$

$$\hat{G}_1 = k_3 \partial_y^2 + k_2 \partial_z^2,$$

$$\hat{G}_2 = \partial_y [k_3 \partial_y^2 + \partial_z^2 + \mathrm{sgn}(\epsilon_a) \pi^2 E_0^2] \tag{10}$$

and

$$\epsilon_d = 1/(\omega\tau_d), \quad \tau_d = \gamma_1 d^2/K_{11}, \quad \gamma_1 = \alpha_3 - \alpha_2,$$

$$\alpha_i' = \alpha_i/\eta_3, \quad \eta_i' = \eta_i/\eta_3, \quad \lambda = \alpha_3/\alpha_2, \quad E_0 = E/E_F,$$

$$\eta_1 = (\alpha_3 + \alpha_4 + \alpha_6)/2, \quad \eta_2 = (\alpha_4 + \alpha_5 - \alpha_2)/2. \tag{11}$$

Here τ_d is the director relaxation time, $k_i = K_{ii}/K_{11}$ with K_{ii} the orientational elastic constants (Frank moduli), $E_F = \pi/d\sqrt{K_{11}/(\epsilon_0|\epsilon_a|)}$ is the Fréedericksz field, and ϵ_a is the anisotropy of the dielectric permittivity.

We also introduce the quantity

$$P_\rho = \tau_v/\tau_d = \rho K_{11}/(\eta_3 \gamma_1), \tag{12}$$

which represents the ratio of the Reynolds number to the Ericksen number and which is of order 10^{-6} for ordinary

nematics. The nematodynamic equations nondimensionalized with the help of Eq. (1) contain the dimensionless parameters ϵ_v and ϵ_d, while all other quantities involve the ratios of the viscosities and elasticities. According to Eqs. (1) and (3) the reduced amplitude $a=A/d$ serves as the main control parameter. It is obvious that the critical flow amplitude a_c at the onset of instability is a universal function, that depends only on the product ωd^2 (or $\omega\tau_d$, since P_ρ is also a material constant).

The boundary conditions (fully rigid) for Eqs. (6)–(9) read

$$v_x|_{z=\pm 1/2}=0, \quad v_z|_{z=\pm 1/2}=v_{z,z}|_{z=\pm 1/2}=0,$$

$$n_x|_{z=\pm 1/2}=0, \quad n_z|_{z=\pm 1/2}=0. \tag{13}$$

We have tested that in the framework of the stability analysis (see below) the inertia term in the velocity equation (3) ($\sim\epsilon_v$) can be neglected, if the frequencies are not too high ($\omega\tau_v \leqslant 1$). Then the solution of Eq. (3) is simply given as

$$v_x^0 = a(z+1/2)\cos t. \tag{14}$$

Let us collect all perturbations in the vector $\mathbf{Y}=(v_x,v_z,n_x,n_z)^{\mathrm{T}}$. From the Floquet theorem one can write the modal solutions of Eqs. (6)–(9) in the form

$$\mathbf{Y} = e^{\sigma t}e^{iqy}\mathbf{y}(z,t), \tag{15}$$

where σ is the growth rate, q is the wave number; $\mathbf{y}(z,t)$ is time periodic with the period of 2π. Instead of solving the Floquet problem (15) directly (for instance by finite difference methods) we employ a Galerkin expansion technique [20]

$$\mathbf{y}(z,t) = \sum_{n=1}^{\infty}\sum_{k=-\infty}^{\infty}\mathbf{c}_{nk}\phi_n(z)e^{ikt}, \tag{16}$$

with constant coefficients $\mathbf{c}_{nk}$. The trial functions $\phi_n(z)$ satisfy the boundary conditions (13). We use Chebyshev polynomials [21]

$$\phi_n(z) = \begin{cases} T_{2m}(2z)-T_0(2z), & n=2m-1, \\ T_{2m+1}(2z)-T_1(2z), & n=2m, \end{cases} \tag{17}$$

for v_x, n_x, and n_z, and for v_z Chandrasekhar functions [22]

$$\phi_n(z) = \begin{cases} \dfrac{\cosh(\lambda_m z)}{\cosh(\lambda_m/2)} - \dfrac{\cos(\lambda_m z)}{\cos(\lambda_m/2)}, & n=2m-1, \\ \dfrac{\sinh(\nu_m z)}{\sinh(\nu_m/2)} - \dfrac{\sin(\nu_m z)}{\sin(\nu_m/2)}, & n=2m. \end{cases} \tag{18}$$

Here λ_m and ν_m are the roots of the appropriate characteristic equations results from $\phi_n(\pm 1/2)=\partial_z\phi_n(\pm 1/2)=0$ [22].

Inspection of Eqs. (6)–(9) shows that the modal solutions (16) have a definite symmetry (even or odd) under the transformations $z\to -z$ and $t\to t+\pi$. Accordingly the possible modes destabilizing the basic state can be classified with the help of symmetry of four types, see Table I. Although we have eliminated the v_y component in the linearized equations it is included in Table I for the completeness. Type I corresponds to the Y symmetry and type II to the Z symmetry in the notations of Pieranski and Guyon [11]. Type-I and -III solutions allow for a nonzero time average of v_y, v_z. In this case rolls are overturning, i.e., they have steadily rotating contribution. Rolls of type II and IV are purely oscillating.

TABLE I. Spatial (z) and temporal (t) symmetries of solutions of linearized Eqs. (6)–(9).

	I		II		III		IV	
	z	t	z	t	z	t	z	t
v_x	even	odd	even	even	odd	odd	odd	even
v_y	odd	even	odd	odd	even	even	even	odd
v_z	even	even	even	odd	odd	even	odd	odd
n_x	even	odd	even	even	odd	odd	odd	even
n_z	even	even	even	odd	odd	even	odd	odd

Substituting Eqs. (15) and (16) into Eqs. (6)–(9) and projecting onto the corresponding Galerkin modes (17) and (18) [20] one obtains a linear, algebraic system for the expansion coefficients $\mathbf{c}_{nk}$ of the form

$$(\mathbf{A}+a\mathbf{B})\mathbf{c} = \sigma\mathbf{C}\cdot\mathbf{c}, \tag{19}$$

where matrices $\mathbf{A}$, $\mathbf{B}$, and $\mathbf{C}$ depend only on the wave number q and the material parameters. Truncating the expansion (16) one can solve the finite dimension eigenvalue problem (19) by standard methods. The condition $\max \mathrm{Re}[\sigma(a,q)]=0$ yields the neutral curve $a_0(q)$. If one assumes a stationary bifurcation, i.e., $\mathrm{Im}(\sigma)=0$ at threshold, then one has to solve the eigenvalue problem

$$(\mathbf{A}^{-1}\cdot\mathbf{B})\mathbf{c} = -\frac{1}{a}\mathbf{c}, \tag{20}$$

which is much more convenient. The minimum of $a_0(q)$ yields the critical wave number $q=q_c$ and the critical flow amplitude $a_c=a_0(q_c)$. Using Eq. (19) we have checked that in all the cases the primary bifurcation of the basic state (2) is stationary.

III. RESULTS AND DISCUSSION

A. Flow induced instabilities without an electric field

The detailed calculations were performed for the material MBBA (4-methoxy-benzylidene-4′-*n*-butylaniline, see Appendix A for the material parameters). The critical amplitude $a_c(\omega\tau_d)$ and the critical wave number $q_c(\omega\tau_d)$ are shown in Fig. 1. For $\omega\tau_d \leqslant 37$ the primary instability in the absence of external fields is homogeneous ($q_c=0$). This could be expected already from the fact that in steady shear flow the homogeneous instability occurs first [11,16]. Interestingly, for $\omega\tau_d > 37$ the primary instability leads to rolls of type I, which persists up to $\omega\tau_d \approx 4.1\times 10^4$. Then there is a transition to rolls of type II. The wave number q_c is about 4.3 at the lowest frequencies and increases monotonously with frequency. At the transition point from type I to type II rolls q_c

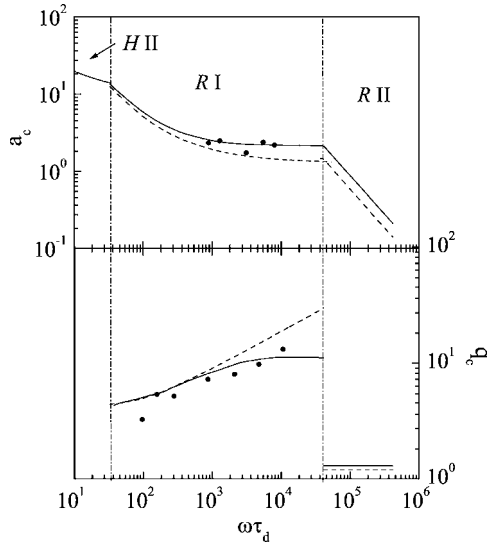

FIG. 1. Critical amplitude a_c and critical wave number q_c vs $\omega\tau_d$ for MBBA. Solid lines are from numerical calculations, dashed lines are obtained from the approximations (24) and (25), points are experimental data from Ref. [13]. *H* denotes homogeneous instability, *R* is roll instability, Roman numbers denote the symmetry type from Table I.

jumps down from 11 to 1.3. We have checked numerically that the appearance of the type II transition is related to the inertia terms in the flow equations (6) and (7), described by the parameter ϵ_v. By neglecting the inertia terms in the Navier-Stokes Eqs. (6) and (7), i.e., for $\epsilon_v \to 0$, the transition was absent. We mention that according to our numerical analysis the thresholds for the instabilities of types III and IV are systematically higher for all frequencies investigated.

In order to clarify the mechanism leading to type I $\to$type II transition we have performed approximate analytical calculations. Applying the operator $(\partial_y^2 - \lambda\partial_z^2)$ on Eq. (7) we eliminate the velocities from Eqs. (8) and (9). In the remaining equations for n_x and n_z we use a one-mode approximation in space

$$n_x = \cos(\pi z)\cos(qy)f(t),$$

$$n_z = \cos(\pi z)\cos(qy)g(t), \tag{21}$$

appropriate for the symmetry of type I or II. After projecting the equations onto the corresponding modes one obtains coupled ODEs for $f(t)$ and $g(t)$. Further simplifications can be made by keeping only the terms in the leading order in $\epsilon_v, \epsilon_v a, \epsilon_d$, while neglecting the terms proportional to $\epsilon_v\partial_t(n_x,n_z)$, $\epsilon_v\partial_t^2(n_x,n_z)$, which are small compared with $\partial_t(n_x,n_z)$. Finally, one arrives at a minimal model that covers all essential features of roll instabilities of type I and II

$$\dot{f} + \epsilon_d m_1 f - (m_2 a\cos t - \epsilon_v m_3 a \sin t)g = 0,$$

$$\dot{g} + \epsilon_d l_1 g - l_2 a \cos t f = 0. \tag{22}$$

The coefficients $m_i(q)$, $l_i(q)$ are given in Appendix B. We look for a solution of Eq. (22), which neither grows nor decays. We assume

$$f = f_{\rm osc}, \quad g = g_{\rm st} + g_{\rm osc}, \quad \text{for type I},$$

$$f = f_{\rm st} + f_{\rm osc}, \quad g = g_{\rm osc}, \quad \text{for type II}, \tag{23}$$

that corresponds to the separation of the functions f and g into the stationary (index st) and oscillatory (osc) parts with time averages $\langle f_{\rm osc}\rangle = \langle g_{\rm osc}\rangle = 0$. Substituting Eq. (23) into Eq. (22) and averaging over the period of the oscillations one obtains the critical amplitudes for roll instabilities of type I and II

$$(a_c^{\rm I})^2 = \frac{2(\epsilon_d^2 m_1^2 + 1)}{[m_1 m_2 + m_3\epsilon_v/\epsilon_d]}\frac{l_1}{l_2}, \tag{24}$$

$$(a_c^{\rm II})^2 = \frac{2(\epsilon_d^2 l_1^2 + 1)}{[l_1 m_2 - m_3\epsilon_v/\epsilon_d]}\frac{m_1}{l_2}. \tag{25}$$

Let us analyze the expressions (24) and (25). From Eqs. (B1) in the Appendix B one finds that $m_1(q)$, $m_2(q)$, $m_3(q)$, and $l_1(q)$ are positive for all q, whereas $l_2(q)$ is positive only for very small $q(\lesssim 0.5)$ and comparatively large $q(\gtrsim 3)$, and negative for q in between. Thus, from Eq. (24) the rolls with symmetry of type I can develop with both $q_c \sim 2\pi$ and $q_c = 0$ (homogeneous instabilities). In Eq. (25) the expression $[m_2 l_1 - m_3\epsilon_v/\epsilon_d]$ in the denominator changes sign from positive to negative with increasing frequency at

$$\omega_{\rm tr}\tau_d = \left[\frac{m_2 l_1}{m_3}\frac{1}{P_\rho}\right]^{1/2}. \tag{26}$$

A lower limit of the transition frequency $\omega_{\rm tr}$ is given by setting $q=0$. For rolls of type II to exist at frequency $\omega > \omega_{\rm tr}$ one needs the negative l_2, which yields an instability with $q_c \sim 1$. Therefore one can conclude from Eq. (25) that only the ratio ϵ_v/ϵ_d plays an essential role in the transition from rolls of type I symmetry to rolls of type II, but not ϵ_v itself.

By increasing $\omega\tau_d$ the critical amplitude $a_c^{\rm I}(\omega\tau_d)$ of mode I given by Eq. (24) appears to tend to a constant value already at rather low values of $\omega\tau_d$, where $\epsilon_v \ll 1$. Such a behavior was described before in Ref. [15], where in a one-mode analysis (spatial and temporal) the inertia terms were completely neglected both for the basic state and for the linear stability problem. One can show that this feature is not an artifact of the one-mode approximation in time. The same result can be obtained by inspecting directly the high-frequency limit in Eq. (22) (see Appendix C).

For the threshold of type II rolls at frequency $\omega\tau_d \gg 1/\sqrt{P_\rho}$, i.e., $\epsilon_v/\epsilon_d \gg 1$, Eq. (25) can be expanded in terms of ϵ_v/ϵ_d that gives

$$a_c^{\rm II} = \left[2\frac{(\epsilon_d^2 l_1^2 + 1)}{m_2 l_1}\frac{m_1}{(-l_2)}P_\rho\right]^{1/2}\epsilon_d. \tag{27}$$

Since $\epsilon_d \ll 1$ for $\omega\tau_d \gg 1$ one sees that $a_c^{\rm II}$ is inversely proportional to $\omega\tau_d$.

The results for the approximate expressions (24) and (25), are included in Fig. 1. Their deviation from the rigorous numerical results is about 30% at small $\omega\tau_d$, and increases with $\omega\tau_d$. This turns out to be a consequence of the spatial

one-mode approximation (21). Nevertheless, the analytic expressions reproduce qualitatively all the important features of the numerically calculated thresholds, including the switching between the modes of types I and II. Note, however, that the frequency dependence of the critical wave number q_c in the one-mode spatial approximation for type I rolls does not show a saturation as in the numerical calculations.

Finally we address the approximation of neglecting the inertia term in velocity equation (3) which leads to simple expression (14) and allows for the minimal model (22). From Eq. (3) at small ϵ_v (for $\omega\tau_d \ll 1/P_\rho \sim 10^6$) one can obtain the correction of the basic velocity (14) as an expansion in ϵ_v. If one keeps only the leading term the threshold amplitude (and, consequently, ω_{tr}) in the numerical calculations changes by less than 10% for $\epsilon_v=0.1$ and the correction becomes smaller at lower frequencies, so that ϵ_v can safely be neglected in Eq. (3) at least up to $\omega\tau_d \sim 10^5$.

B. Comparison with experiments

In the experiments of PG with the nematic MBBA layer of thickness $d=240$ μm rolls of type I have been observed as the first instability at critical amplitude a_c varying from 4.5 to 2.5 for frequency changing from $\omega\tau_d=2.9\times10^3$ to $\omega\tau_d=1.1\times10^4$ with critical wave number $q_c \approx 2\pi$ [11]. These numbers were very close to those found in our calculations, but one should note that in the experiments a constant magnetic field has been used in order to stabilize the initial director orientation (the study of the influence of a magnetic field on the flow instabilities is beyond the scope of present work).

Oscillatory Couette flow was investigated experimentally also by Anikeev and Kapustina [13]. The authors used an eutectic mixture of MBBA and EBBA, which is supposed to have almost the same material parameters as MBBA. A geometry where the director is anchored in the plane of the layer at an angle ψ to the shear direction was investigated. For the case $\psi=90°$, in which we are interested in, the frequency dependence of a_c and q_c were given for $d=90$ μm. The experimental points taken from [13] are included in Fig. 1. The agreement between experimental and theoretical data is good.

Experiments of Mullin and Peacock [14] performed with the nematic E7 show the existence of a roll instability at least up to 150 Hz with d between 20 and 50 μm. A good test for the quality of oscillatory Couette flow experiments is the scaling law $a_c=F(\omega\tau_d)$, where F is determined from the nematodynamic equations. The experimental data of Mullin and Peacock pass this test only in a rather narrow region at low frequencies, namely, up to about 40 Hz for $d=20$, 30, and 40 μm. At higher frequencies the scaling law is of variance with the experiments and the data follows more a relation similar to $a_c=F(\omega)$. This feature could be caused by failure of the surface anchoring and/or departures from Couette flow in the experimental setup. Mullin and Peacock report, that the observation of probe particles has revealed no average flow, which could mean that the rolls are of type II, the purely oscillating, characterized by a vanishing time average of velocity. On the other hand in the experiments the critical wave number increases with increasing oscillatory flow frequency whereas for rolls of type II one would expect that q_c remains nearly constant (see Fig. 1).

TABLE II. For the standard values of the material parameters of MBBA at 25 °C and $\omega\tau_d=825$ (typical value for lowest frequencies in experiments [14]) the roll instability of type I (overturning rolls) takes place at critical amplitude $a_c=2.6$ and critical wave number $q_c=7$. When any one of the parameters is varied alone, a transition to type II (oscillating rolls) occurs at the value given in the third column. In the fourth and fifth columns the new values of the threshold amplitude and the critical wave number are given.

	Standard values	Transition values	New a_c	New q_c
α_1/α_2	0.164	1.01	2.38	6.9
α_4/α_2	−0.748	−5.92	7.72	10.1
α_5/α_2	−0.706	−1.83	6.64	1.4
α_6/α_2	0.304	−0.85	6.60	1.4
K_{11}/K_{22}	1.586	5.95	2.93	7.3
K_{33}/K_{22}	2.05	0.15	1.66	16.6

We have found in the literature only the values of the elastic constants for E7 [23], thus we are not able to perform a direct comparison of our theoretical results with the experimental data from Ref. [14]. Instead, we have explored the impact of variation of the material parameters on the instability type. The results of this study are presented in Table II. Although we have in fact identified the possibility of the rolls of type II at low frequencies for a certain (reasonable) set of the material parameters, the discrepancy in frequency dependence of the critical wave number remains.

C. Influence of an electric field on the instability type and symmetry

Applying an electric field across the nematic layer can lead to switching between different types of temporal symmetry of rolls induced by oscillatory shear flow. In the case of MBBA the change of the roll instability of type I to type II by increasing the electric field strength was observed [11]. We have performed the stability analysis of the linearized equations (6)–(9) in a wide range of the oscillatory flow frequency and electric field strength for MBBA, which has a *negative* anisotropy of the dielectric permittivity. We have found that the electric field can change not only the temporal symmetry of the instability, but also the spatial symmetry: the phase diagram (Fig. 2) presents the regions, where the rolls with symmetry type III appear at the threshold. According to their spatial symmetry these rolls represent a double-layered structure, so that the critical wave number in this area is about two times larger than in "normal," one-layered rolls. For low values of $\omega\tau_d$ the applied electric field leads to an increase of the region of homogeneous instability (H), which means that the electric field suppresses the roll instability. The profiles of the velocity and the director for various modes with different symmetry are plotted in Fig. 3.

We have also calculated the phase diagram for a nematic with positive dielectric anisotropy (Fig. 4). The material pa-

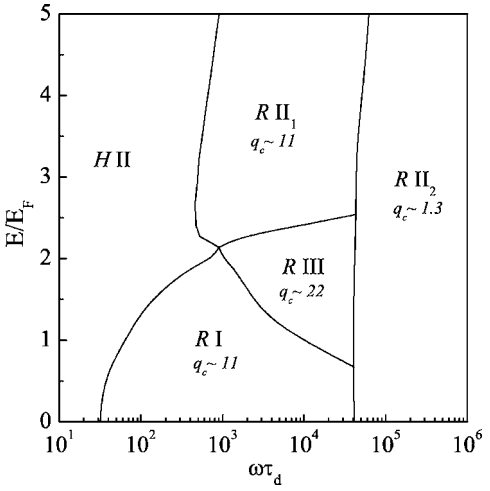

FIG. 2. Phase diagram of instabilities induced by oscillatory Couette flow in the presence of an electric field for a nematic with *negative* dielectric anisotropy. *H* denotes homogeneous instability, *R* is roll instability, Roman numbers denote the group of symmetry from Table I.

rameters were taken from MBBA except $\epsilon_a = |\epsilon_a^{\mathrm{MBBA}}|$. In this case the phase diagram (Fig. 4) presents quite large region of rolls of symmetry type I. At low $\omega\tau_d$ there is a switching between homogeneous instabilities of types I and II when varying the electric field. Note, that under these conditions without flow the splay Fréedericksz transition takes place at $E/E_F=1$, which leads to a homogeneous distortion predominantly at the middle of the nematic layer. As a result, when in the presence of Couette flow the applied electric field E approaches E_F, a cooperative effect is expected and in fact the critical flow amplitude a_c goes to zero. The one-mode analysis in this case does not agree very well with the full numerical calculations, although it keeps all the important features (switching between modes, etc.).

IV. CONCLUSION

We have obtained the complete phase diagram of the orientational instabilities, both homogeneous and spatially periodic, in a flow aligning nematic liquid crystal subjected to oscillatory Couette flow in the geometry, where the director is prealigned perpendicular to the flow plane (spanned by the primary flow velocity and its gradient). A linear stability analysis of the full set of the nematodynamic equations has been carried out. It has been found that the inertia effects of the nematic fluid, usually neglected in the theoretical considerations, are responsible for a new type of roll instability and for the switching between roll instabilities of different temporal symmetry. The important role of inertia effects has been clearly borne out by analytical calculations. The agreement between numerical simulations of the underlying equations and available experimental data is good.

For the nematic liquid crystal MBBA increase of the flow frequency leads to the transition between rolls of symmetry types I and II. Both of these modes can easily be distinguished in experiments. For MBBA material parameters one has the transition at $\omega\tau_d \approx 4.1\times 10^4$. For $d=240$ μm, the value used in the PG experiments [11], this corresponds to $f\approx 7$ Hz. The maximal frequency in this experiment was ~ 2.5 Hz, so the effect could not be observed. Recent experiments on oscillatory Couette flow in nematics [13,14] demonstrate techniques to study the high-frequency range in detail.

We have also investigated the effect of an additional electric field applied across the nematic layer for liquid crystals with negative and positive dielectric anisotropy. For MBBA it was found that the electric field causes a transition to a double-layered roll structure [*R* III, Fig. 3(d)] in a regime, which is intermediate between that of rolls of types I and II. In this case, the critical wave number is about twice of those of "normal" rolls (*R* I and *R* II_1). Another interesting point in the experimental investigations could be the transition between rolls of the same symmetry but quite different wave numbers by increasing the flow frequency at $E/E_F>3$ (*R* $\mathrm{II}_1 \rightarrow R\ \mathrm{II}_2$ in Fig. 2).

ACKNOWLEDGMENTS

We wish to thank T. Mullin and T. Peacock for communicating us their results before publication and W. Pesch for helpful discussions and critical reading of manuscript. Financial support by DFG (Grants Nos. Kr690/14-1, Kr690/22-1) and RFBR (Grants Nos. 05-02-16716, 05-02-16548, 05-02-97907) are gratefully acknowledged.

APPENDIX A

Material parameters of nematic liquid crystal MBBA (at 25 °C) used in numerical calculations [24,25]. Elastic constants $K_{11}=6.66$, $K_{22}=4.2$, $K_{33}=8.61$ (in units 10^{-12} N); viscosity coefficients $\alpha_1=-18.1$, $\alpha_2=-110.4$, $\alpha_3=-1.1$, $\alpha_4=82.6$, $\alpha_5=77.9$, $\alpha_6=-33.6$ (in units 10^{-3} N s/m^2); anisotropy of the dielectric permittivity $\epsilon_a=-0.53$.

APPENDIX B

The coefficients $m_i(q)$, $l_i(q)$ in Eq. (22)

$$m_1 = (\eta_2' q^2 + \pi^2)(k_3 q^2 + k_2 \pi^2)/r_1,$$

$$m_2 = [(\eta_2' - c_1) q^2 + \pi^2]/[r_1(1-\lambda)],$$

$$m_3 = 1/[r_1(1-\lambda)],$$

$$l_1 = r_2[k_3 q^2 + \pi^2 - \mathrm{sgn}(\epsilon_a)\pi^2 E_0^2]/r_3,$$

$$l_2 = [\lambda r_2 - (q^2 - \lambda\pi^2)(c_2 q^2 - c_3 \pi^2)]/[r_3(1-\lambda)], \quad \text{(B1)}$$

with

$$r_1 = [\eta_2' + (1-\lambda)^{-1}\alpha_2']q^2 + \pi^2,$$

$$r_2 = [\eta_2' q^2 + (\alpha_1' + \eta_1' + \eta_2')\pi^2]q^2 + \eta_1' \pi^4,$$

$$r_3 = r_2 + (1-\lambda)^{-1}\alpha_2'(q^2 - \lambda\pi^2)^2,$$

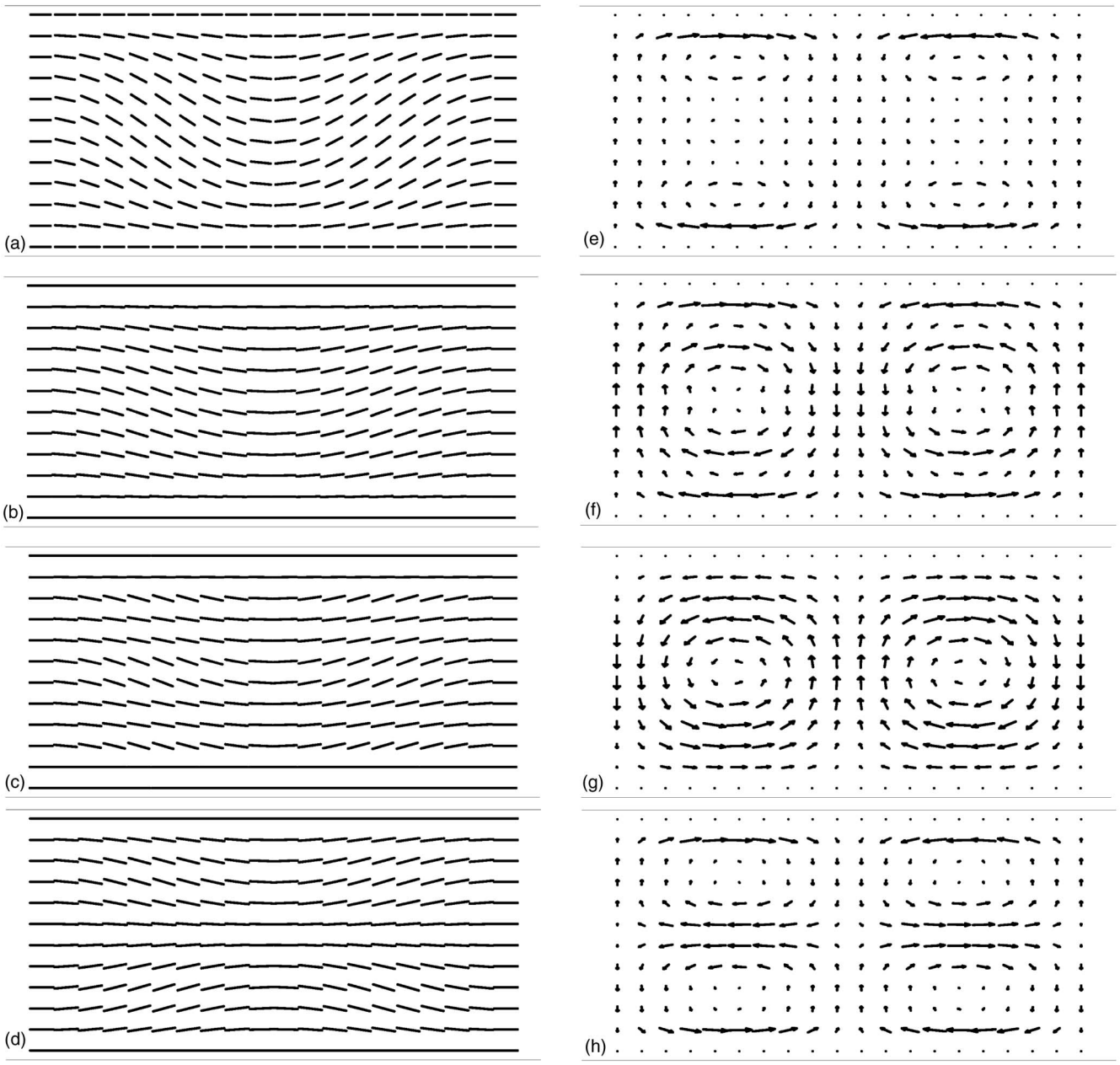

FIG. 3. Director (left) and velocity (right) profiles, cross section in the y-z plane: (a) R I, time averaged, $q_c \sim 11$; (b) R II$_1$, $t=0$, $q_c \sim 11$; (c) R II$_2$, $t=0$, $q_c \sim 1.3$; (d) R III, time averaged, $q_c \sim 22$.

$$c_1 = \tfrac{1}{2}(-\alpha_2' + \alpha_5'),$$

$$c_2 = \tfrac{1}{2}(\alpha_2' + \alpha_5'),$$

$$c_3 = \tfrac{1}{2}(\alpha_3' + \alpha_6').$$

APPENDIX C

To investigate the behavior of the critical amplitude in the high-frequency range we neglect ϵ_v in Eq. (22) and expand the functions f and g in small parameter $\epsilon_d = 1/(\omega\tau_d)$. Formally this analysis is valid for $1 \ll \omega\tau_d \ll 1/P_\rho$. Then equations (22) can be written in the matrix form

$$\frac{d}{dt}\mathbf{Y} = \mathbf{A}(t)\mathbf{Y}, \tag{C1}$$

where

$$\mathbf{Y} = \begin{pmatrix} f \\ g \end{pmatrix}, \quad \mathbf{A} = \begin{pmatrix} -\epsilon_d m_1 & m_2 a \cos t \\ l_2 a \cos t & -\epsilon_d l_1 \end{pmatrix}.$$

The treatment follows the well known procedure of time-dependent perturbation theory in quantum mechanics. We seek a periodic solution of Eq. (C1) of the form

$$\mathbf{Y} = \mathbf{Y}_0 + \epsilon_d \mathbf{Y}_1 + \cdots .$$

At zero order in ϵ_d one has

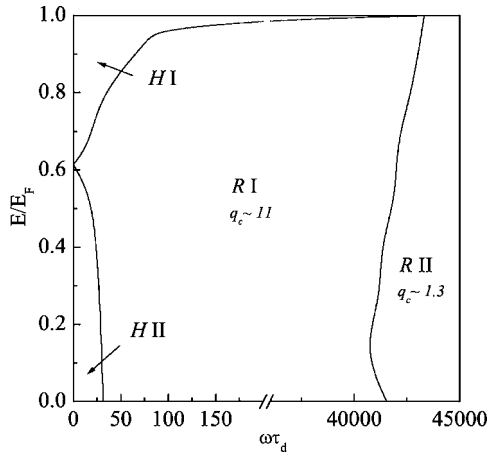

FIG. 4. Phase diagram of instabilities induced by oscillatory Couette flow in the presence of an electric field for a nematic with *positive* dielectric anisotropy. *H* denotes homogeneous instability, *R* is roll instability, Roman numbers denote the group of symmetry from Table I.

$$\frac{d}{dt}\mathbf{Y}_0 = \mathbf{A}_0(t)\mathbf{Y}_0, \tag{C2}$$

where $\mathbf{A}_0=\mathbf{A}(\epsilon_d=0)$. Since $\mathbf{A}_0(t)$ commutes with $\mathbf{A}_0(t')$ (in contrast to $\mathbf{A}$) the solution of the matrix equation (C2) has the form

$$\mathbf{Y}_0 = e^{\int_0^t d\tau \mathbf{A}_0(\tau)}\mathbf{Y}^0, \quad \mathbf{Y}^0 = \begin{pmatrix} f^0 \\ g^0 \end{pmatrix}, \tag{C3}$$

where f^0 and g^0 are initial values (fluctuations) of the functions f_0 and g_0, respectively. It can easily be seen, that $\mathbf{Y}_0$ is periodic with time averages $\langle f_0\rangle \sim f^0$, $\langle g_0\rangle \sim g^0$, so that the state with $(f^0=0, g^0\neq 0)$ corresponds to the mode of symmetry type I, and the state $(f^0\neq 0, g^0=0)$ corresponds to mode of symmetry type II.

At the first order in ϵ_d one has the system

$$\frac{d\mathbf{Y}_1}{dt} = \mathbf{A}_0(t)\mathbf{Y}_1 + \mathbf{b}, \quad \text{with } \mathbf{b} = \begin{pmatrix} -m_1 f_0 \\ -l_1 g_0 \end{pmatrix}. \tag{C4}$$

The solution of Eq. (C4) is given by

$$\mathbf{Y}_1 = \mathbf{Y}_0 + e^{\int_0^t d\tau \mathbf{A}_0(\tau)} \int_0^t d\tau e^{-\int_0^\tau d\xi \mathbf{A}_0(\xi)} \mathbf{b}(\tau). \tag{C5}$$

Substituting $\mathbf{b}$ into Eq. (C5) and using the relation [21]

$$e^{z\sin\theta} = I_0(z) + 2\sum_{k=0}^{\infty} (-1)^k I_{2k+1}(z)\sin[(2k+1)\theta]$$

$$+ 2\sum_{k=1}^{\infty} (-1)^k I_{2k}(z)\cos(2k\theta),$$

where I_i are modified Bessel functions of integer order, one has the periodicity condition for $\mathbf{Y}_1$

$$I_0(2\sqrt{m_2 l_2}a) = -\frac{l_1+m_1}{l_1-m_1} \quad \text{for I type}, \tag{C6}$$

$$I_0(2\sqrt{m_2 l_2}a) = \frac{l_1+m_1}{l_1-m_1} \quad \text{for II type}. \tag{C7}$$

Equations (C6) and (C7) represent the connection between the flow amplitude a and the wave number q in the implicit form. Solving these equations (numerically) one gets the neutral curve $a_0(q)$. Minimization of $a_0(q)$ gives the critical values of the flow amplitudes a_c and the wave number q_c.

Equation (C7) has no real roots for $q \geqslant 0.5$, so that when the fluid inertia term is neglected, only a roll instability of symmetry type I or homogeneous instability of symmetry type II can develop. Equation (C6) gives a critical amplitude $a_c \approx 2.2$ and wave number $q_c \approx 12$, which is in a good agreement with the numerical results (see Fig. 1). From Eq. (C7) it follows that the smallest threshold $a_c \approx 10.9$ corresponds to $q_c=0$.

The above analysis shows the role of the elasticity described by terms proportional to ϵ_d in the nematodynamic equations. The nature of these terms is singular, i.e., when these terms are neglected the critical flow amplitude vanishes $(a_c=0)$, although for infinitesimal ϵ_d there exists a finite value of a_c. Another point is that at high enough frequencies a_c does not depend on the flow frequency, which is in contrast to the case of director alignment within the flow plane [5], where the critical amplitude of the roll instability monotonically decreases with the flow frequency.

[1] P. G. de Gennes and J. Prost, *The Physics of Liquid Crystals* (Clarendon Press, Oxford, 1993).
[2] E. Dubois-Violette, and P. Manneville, in *Pattern Formation in Liquid Crystals*, edited by A. Buka and L. Kramer (Springer-Verlag, New York, 1996), Chap. 4, p. 91.
[3] A. D. Rey and M. M. Denn, Annu. Rev. Fluid Mech. **34**, 233 (2002).
[4] I. Zuniga and F. M. Leslie, Liq. Cryst. **5**, 725 (1989).
[5] A. P. Krekhov, T. Börzsönyi, P. Tóth, A. Buka, and L. Kramer, Phys. Rep. **337**, 171 (2000).
[6] F. M. Leslie, Adv. Liq. Cryst. **4**, 713 (1979).
[7] S. A. Pikin, Zh. Eksp. Teor. Fiz. **65**, 2495 (1973) [Sov. Phys. JETP **38**, 1246 (1974)].
[8] S. A. Pikin and V. G. Chigrinov, Zh. Eksp. Teor. Fiz. **67**, 2280 (1974) [Sov. Phys. JETP **40**, 1131 (1975)].
[9] A. P. Krekhov and L. Kramer, Phys. Rev. E **53**, 4925 (1996) J. Phys. II **4**, 677 (1994).
[10] O. S. Tarasov and A. P. Krekhov, Crystallogr. Rep. **44**, 1121 (1999).
[11] P. Pieranski and E. Guyon, Phys. Rev. A **9**, 404 (1974).
[12] E. Guyon and P. Pieranski, J. Phys. (France) **36**, C1-203 (1975).
[13] D. I. Anikeev and O. A. Kapustina, Zh. Eksp. Teor. Fiz. **110**, 1328 (1996) [JETP **83**, 731 (1996)].

[14] T. Mullin and T. Peacock, Proc. R. Soc. London, Ser. A **455**, 2635 (1999).
[15] E. Dubois-Violette, E. Guyon, I. Janossy, P. Pieranski, and P. Manneville, J. Mec. **16**, 733 (1977).
[16] P. Manneville and E. Dubois-Violette, J. Phys. (France) **37**, 285 (1976).
[17] P. Manneville and E. Dubois-Violette, J. Phys. (France) **37**, 1115 (1976).
[18] I. Janossy, P. Pieranski, and E. Guyon, J. Phys. (France) **37**, 1105 (1976).
[19] P. Manneville, J. Phys. (France) **40**, 713 (1979).
[20] D. Gottlieb and S. A. Orszag, *Numerical Analysis of Spectral Methods: Theory and Applications* (Capital City Press, Montpelier, 1993).
[21] M. Abramowitz and I. A. Stegun, *Handbook of Mathematical Functions* (Dover, New York, 1970).
[22] S. Chandrasekhar, *Hydrodynamic and Hydromagnetic Stability* (Oxford University Press, Oxford, 1961).
[23] F. Yang, J. R. Sambles, and G. W. Bradberry, J. Appl. Phys. **85**, 728 (1999); F. Yang, J. R. Sambles, Y. Dong, and H. Gao, *ibid.* **87**, 2726 (2000).
[24] W. H. de Jeu, W. A. P. Claassen, and A. M. J. Spruijt, Mol. Cryst. Liq. Cryst. **37**, 269 (1976).
[25] H. Kneppe, F. Schneider, and N. K. Sharma, J. Chem. Phys. **77**, 3203 (1982).